Al-Furat Journal of Innovations in Electronics and Computer Engineering (FJIECE)
ISSN -2708-3985

Utilizing Elliptical Ring IMI-Plasmonic Waveguides, Nanomaterials in Nanophotonic Structure for All-Optical 2 × 1 Demultiplexer

Mohammed Sabah Talib[*], Faris Al-Jaafiry

Engineering Technical College-Najaf, Al-Furat Al-Awsat Technical University, 31001 Najaf, Iraq.
Najaf, Iraq.
[*]mohammed.ms.etcn31@student.atu.edu.iq

https://doi.org/10.46649/fjiece.v3.2.30a.9.6.2024

Abstract. *In many industries, particularly electronics, photonic devices are indispensable. However, the diffraction limit and miniaturization are the two problems that have hampered the development of photonics devices. These problems are resolved by plasmonic devices, which enable nanophononics and nanodevices. One of the primary all-optical demultiplexer components utilized in an all-optical Athematic Logic Unit (ALU), which is regarded as the basic building block for all-optical computers, is a plasmonic demultiplexer This paper provides a new design for an elliptical ring insulator-metal-insulator (IMI) plasmonic waveguide-based all-optical demultiplexer (Demux). The suggested device has a small footprint (300 nm × 250 nm) and works at a 1550 nm wavelength. Demux has a 0.5 transmission threshold between logic zero and logic one states. Transmission (T), extinction ratio (contrast ratio (CR)), modulation depth (MD), and insertion loss (IL) are the four metrics that best explain the performance of the plasmonic Demux. The suggested structural dimensions are outstanding and optimal based on the values of MD for Demux which is (95.87%). The device's maximum transmission efficiency is 56.84%. The suggested plasmonic Demux structure makes a substantial contribution to all-optical signal processing Nano-circuits and nano-photonics integrated circuits. Using COMSOL Multiphysics, we simulate the proposed plasmonic Demux using the Finite Element Method (FEM).*

Keywords: *2×1 Demultiplexer; plasmonic; SSP;* Demux*; Transmutation.*

1. INTRODUCTION

Surface Plasmon Polaritons (SPPs) have drawn the attention of researchers working on integrated circuit design for years. SPPs depict the propagation of electromagnetic plane waves and free metal electrons interacting at the dielectric metal contact [1-5]. The primary issues with traditional electrical devices are delay and significant heat generation; also, the diffraction limit is a difficulty with photonic devices. This can be resolved by utilizing plasmonic devices, which provide a way to get beyond the drawbacks of traditional electrical and optical technologies [6-7]. The fundamental principle underlying the construction of plasmonic devices is to control Light signals in plasmonic waveguides can interact with one another both constructively and destructively [7-8]. Many passive and active SPPs devices, including multiplexer and demultiplexers [8-10], sensors [11, 12], switches [13, 14], nanowires [15, 16], splitters [17], filters [18,19], couplers [20], resonators [21] and demultiplexers [22], have recently been developed. Plasmonic waveguides using metal-insulator-metal (MIM) and insulator-metal-insulator (IMI) configurations are the two most common forms of plasmonic waveguides employed in these works. IMI waveguides are simpler to fabricate and have greater propagation length and reduced propagation loss [9].

in Ref. [31], Researchers created a miniature device that uses a metal-insulator-metal (MIM) structure to divide light signals into four distinct wavelengths. With a threshold of about 0.42, it functions well at two wavelengths: 1490 nm and 1520 nm. There are certain restrictions, though. Only demultiplexing (separating signals) is the design's present emphasis, and its relatively large size (1.4 µm × 1.2 µm) and mediocre maximum transmission efficiency of 50% may make fabrication difficult.

In [32], Researchers designed a tiny, all-optical device by using a Plasmonic MIM waveguide. This demultiplexer achieves a Low transmission efficiency (45%) and is extremely compact. However, the design is focused on its function as a demultiplexer, and the study only evaluates its transmission and contrast ratio.

In [33], This research introduces a Drude model and demultiplexer built with special light-guiding structures (dielectric-loaded plasmonic waveguides). Designed for a wavelength of 1074 nm and 1307 nm, The design achieves transmission signal calculation only.

To achieve a 1×2 demultiplexer in structure, a system where three straight waveguides are connected to IMI plasmonic waveguides with elliptical rings with a high transmission ratio and acceptable contrast ratio is suggested in this study. The operating wavelength is 1550 nm, and the planned structure has a tiny dimension of (300 nm× 250 nm). COMSOL Multiphysics 5.4 software is used to perform FEM to provide the numerical results. The suggested plasmonic demultiplexer may be used in Arithmetic Logic Unit (ALU) architecture with all-optical nano-circuits for signal processing.

The format of this article is as follows: The intended structure is described in Section 2; Section 3 discusses the analysis and simulation results and highlights the main strengths of this work through comparisons with previous related studies; Section 4 presents the conclusions of this research and highlights the main strengths of this work through comparisons with previous related studies.

2. THE PROPOSED LAYOUT AND THEORETICAL CONCEPT

Metal-insulator-metal (MIM) and insulator-metal-insulator (IMI) plasmonic waveguides are the two waveguide types that have been utilized most frequently in recent applications. IMI waveguides are easier to fabricate, have a longer propagation length, and have reduced propagation loss [9]. As a result, we decided on IMI plasmonic waveguides as opposed to MIM plasmonic waveguides.

To create a demultiplexer (Demux), Three straight stripes and a single nano-ring resonator are required by our suggested design. As shown in **Figure 1**, this design is based on the insulator metal insulator (IMI). The two materials used in the suggested design are zircon, which makes up the remaining portion of the structure, and silver, which is used to make the nano-ring resonator and the straight stripes. With a refractive index of 2.015, zinc oxide (ZnO) [23], we utilized the to define the silver permittivity, use data from Johnson and Christy [24].

Al-Furat Journal of Innovations in Electronics and Computer Engineering (FJIECE)
ISSN -2708-3985

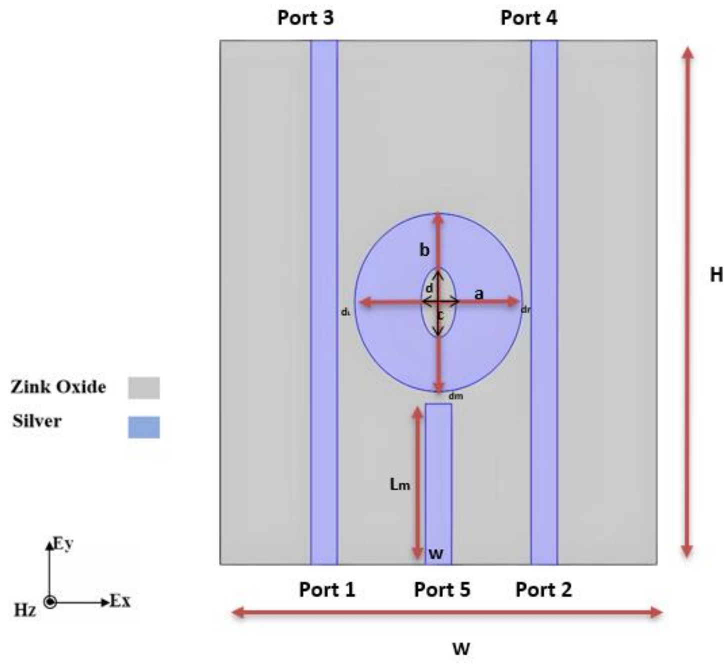

Figure 1. Structure's proposed plasmonic 1×2 Demux with 300 nm × 250 nm area.

Table 1. The suggested structure's parameters.)

Parameter	Description	Value (nm)
H	High of structure	300
W	Width of structure	250
Lm	Length of middle stripes	94
b	Large diameter b	55
a	Small diameter a	48
w	Width of stripes	15
dL	Distance between left stripe and Ellipse Disc	10
dm	Distance between middle stripe and Ellipse Disc	5
dr	Distance between right stripe and Ellipse Disc	5

For applications involving optical communication, 1550 nm is the ideal wavelength which is why it was selected.

When the phase of the selector signal and both inputs are the same, constructive interference happens.

On the other hand, if the light wave phases of the inputs and the selector signal differ, destructive interference will happen.

Based on equation (1) [25], we deduce that the waves interact destructively with one another as a result of the phase difference [26].

$$m = (4n_{eff}\, d \cos\theta)/\lambda \qquad (1)$$

where λ is the wavelength of the incident light wave, d is the silver's thickness, m is the interference order, stated as an integer greater than 0, and θ is the light wave phase.

Al-Furat Journal of Innovations in Electronics and Computer Engineering (FJIECE)
ISSN -2708-3985

To achieve improved modulation depth, high contrast ratio, low insertion loss, and better transmission, the input(s), output(s), and selector ports are chosen using the trial-and-error method. The first and second ports in Demux will be input and selector ports, respectively (S, Y) and the output ports will be ports 3 and 4 (B, A). port 5 will always be in the ON state to maintain the balance of the design. Four factors influence the quality of the plasmonic Demux: insertion loss (IL), modulation depth (MD), transmission (T), and contrast ratio (CR). The transmission is linked to the optical power that is moved from the input ports to the output ports.

It is defined as equation (2) [27]:

$$\mathrm{T} = \left(\frac{Pout}{Pin} \right) \qquad (2)$$

With T standing for transmission at ports (1, 2, and 5) in Demux, the pin can be thought of as the input power. Pout is the term used to describe the optical output power in Demux at ports 3 and 4. Applying this equation results in the output state of the necessary structure while considering the threshold value. Considering that the suggested structure's threshold value is 0.5, The state of output will be logic 1 (ON) if the ratio result exceeds the threshold limit and logic 0 if it falls below the threshold limit (OFF).
The optical power output in the ON and OFF states (Pout |ON and Pout |OFF, respectively) are compared to determine the contrast ratio (CR), which is the second parameter.

$$\mathrm{CR\ (dB)} = 10\log\left(\frac{Pout\,|\,ON_{\min}}{Pout\,|\,OFF_{\max}} \right) \qquad (3)$$

When the contrast ratio is higher, it means that the intended structure is operating more effectively. The description of CR's value depends on [27]. The connection between the highest transmission during the ON state (TON|Max) and the OFF state's little transmission (TOFF|Min) is represented by the third parameter, the depth of modulation (MD). It is described as follows in [28]

$$\text{Modulation depth(MD)} = \left(\frac{MaxT_{ON} - MinT_{OFF}}{MaxT_{ON}} \right) \qquad (4)$$

This ratio establishes the optimality of the dimensions chosen for the suggested design. In light of [28], the values described by MD were obtained. The fourth parameter, insertion loss (IL), is calculated from equation (4) [29] It is linked to the optical power input listed in **Table 2** as well as the lowest optical output power that may be achieved when turned ON.

$$\mathrm{IL\ (dB)} = -10\log\left(\frac{Pout\ \,|\,ON_{\min}}{Pin} \right) \qquad (5)$$

This parameter evaluates the losses caused by the insertion of one device into another.

Table 2. Describe the Insertion Loss values [30]

IL (dB) ranges	Description	Assessment of IL
More than 5	Very High	Bad and Inefficient
More than 3 - 5	High	Accepted
More than 1 - 3	Medium	Moderate
More than 0 - 1	Low	Good
More than -1 - 0	Very Low	Very Good and Efficient
-1 and less	Ultra-Low	Excellent and Efficient

3. RESULTS AND DISCUSSION

Al-Furat Journal of Innovations in Electronics and Computer Engineering (FJIECE)
ISSN -2708-3985

Figure 3 demonstrates how the suggested structure is lighted to investigate the Demux effect by a plane wave having a wavelength between 1350 and 1750 nm. The typical symbol and truth table for a 1×2 Demux is shown in **Figure 2 (a, b)**, correspondingly. While the input and selector ports (ports 2 and 1, respectively) are envisioned to be in the Y and S states, Port 5 is always in the ON state in the proposed Demux. It is expected that the output ports (ports 4 and 3, respectively) are in the A and B states.

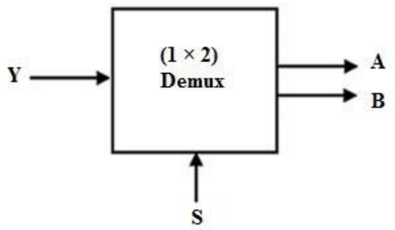

(a)

S (port 1)	Y (port 2)	A (port 4)	B (port 3)
0	0	0	0
0	1	1	0
1	0	0	0
1	1	0	1

(b)

Figure 2. Demultiplexers: (a) conventional symbol; (b) truth table.

The input port (Y), selector port (S), and output ports (A and B) of the demultiplexer are all in the off (OFF) state, as shown in **Figure 3**. Conversely, when the input port (Y) is ON, the output ports (A and B) will be off and on, respectively.

The transmission values at 1550 nm wavelength for ports A and B, respectively, are 0.0479 and 0.0289, according to the data, and these transmissions are below the transmission threshold. The transmission values in ports A and B at the operating wavelength are respectively 0.7013 and 0.3291 after the single input port has been activated. Destructive interference between the two ports will occur when the input port is shut off and the selection port is switched on with a 180-degree phase, as shown in **Figure 3**. Afterward, both A and B's output ports will be in the OFF state; in this instance, port A's transmission is 0.1281 and port B's transmission is 0.0732. Additionally,

The Y port is 180 degrees in phase., the transmission in ports A and B is 0.1002 and 0.5648, and the input and selection port is in the ON state. This structure's modulation depth is 95.87 percent, and its contrast ratio is 2.3456 dB and 2.48 dB are lost in the insertion.

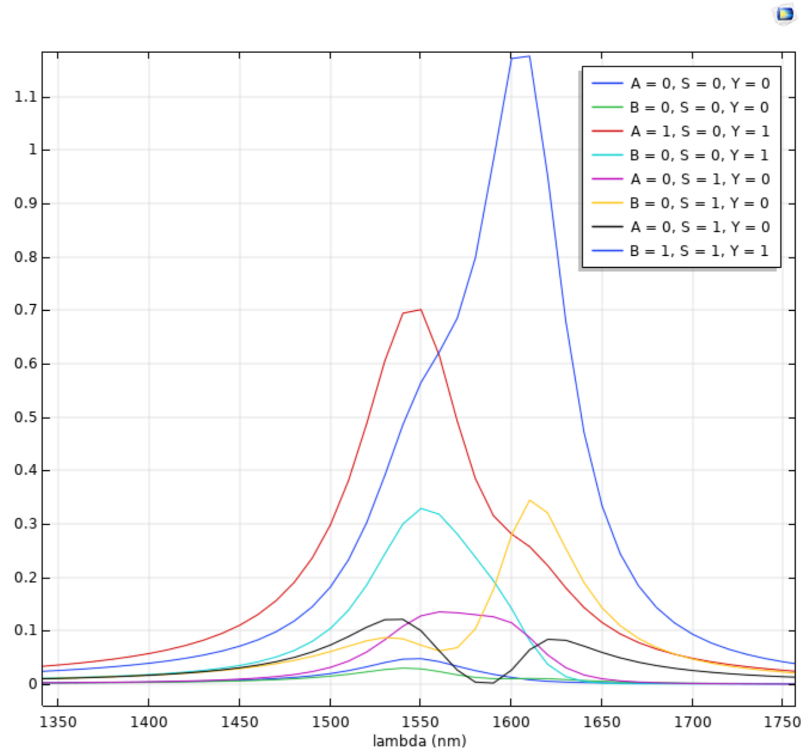

Figure 3. The suggested plasmonic Demux transmission spectrum in various stages.

Table 3 shows that the modulation depth is quite great and that the transmission threshold is ideal because there is a noticeable discrepancy between the ON state's maximum transmission and the OFF state's minimum transmission. As a result, [28] asserts that the proportions of the suggested building are excellent and perfect. Additionally, after that, both A and B's output ports will be in the OFF state; because the ON state's lowest optical output power is somewhat higher than the OFF state's maximum optical output power. **Table 2** further shows that the IL is mild.

Table 3. Summarized simulation results in Fig. 3

S (port1)	Y (port2)	A (port4)	B (port3)	T at A	T at B	MD (%)	CR (dB)	IL (dB)	T threshold
0	0	0	0	0.0479	0.0289	95.87%	2.3456	2.48	0.5
0	1	1	0	0.7013	0.3291				
1	0	0	0	0.1281	0.0732				
1	1	0	1	0.1002	0.5648				

With the input port and selection switched ON, the magnetic field distribution (Hz-component) is shown in **Figure 4(a)**. On the other hand**, Figure 4(b)** displays the magnetic field distribution when the input port and selection are both enabled. A change in color from blue to red denotes a high to low level of light power intensity. **Figure 4's** color-coded bar illustrates this variation in light power intensity**.**

Al-Furat Journal of Innovations in Electronics and Computer Engineering (FJIECE)
ISSN -2708-3985

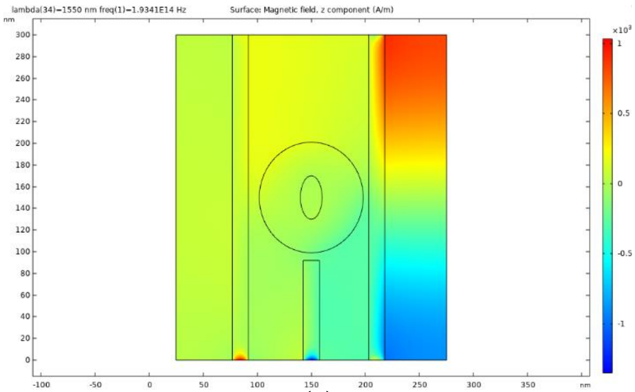

(a)

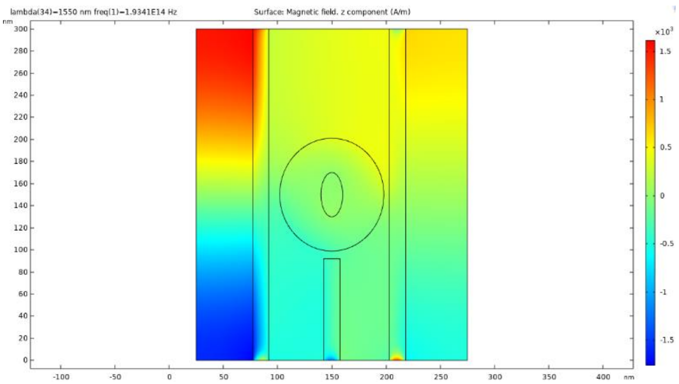

(b)

Figure 4. The magnetic field distribution (Hz-component) when: (a) S is ON, B and A are OFF states, the output Y is OFF states; (b) S, A and B are ON states, the output Y is ON states.

THIS WORK'S COMPARISON WITH OTHERS FROM THE LAST DECADE

The main characteristics of the suggested plasmonic demultiplexer are contrasted with those of earlier attempts in **Table 4.**

Table 4. Comparison of differences between our structure and previous works.

Topology	Size	Metal Model	Threshold limit	Operating wavelength	Performance Measured By	Max Tran.	Structure Complexity	Ref
Nano ring IMI Nano plasmonic waveguides	300 nm × 250 nm	Johnson and Christy's data	0.5	1550 nm	Four parameters (T, CR, MD, IL)	56.48%	Less	This work
Plasmonic slot resonator	1.4 μm ×1.2 μm	Drude model	0.4	1490 nm, 1520 nm	One parameter (T)	52%	More	Ref [31]

Plasmonic MIM waveguide	2 μm ×1.5 μm	Drude model	0.1	1550 nm, 1400 nm	Three Parameters (T, CR, XT)	45%	More	Ref [32]
(MIM) waveguide	More than 560 nm × 500 nm	Drude model	0.5	1074 nm, 1307 nm	One parameter (T)	56%	More	Ref [36]

4. CONCLUSIONS

This paper demonstrates why plasmonic technology is among the finest options for reducing the size of optical devices used in communications. were created: a single structure with identical dimensions, a single wavelength, and a single transmission threshold housing a demultiplexer. COMSOL MULTIPHSICES 5.4 was used for numerical analysis of the data, When the propagating signals in the inputs and control port are implemented using the optical interference characteristic, as well as the coupling process between the waveguides and the slot cavities, served as the foundation for these multiplexers and demultiplexers. According to the modeling findings, this structure suggests the ellipse ring has dimensions of (300 × 250) nm and maximum transmission of (56.87 %) in the Demultiplexer, and the highest contrast ratio was (2.3 dB) and modulation depth (98.20%) and (2.48) dB are lost in the insertion.

REFERENCES

[1] Bozhevolnyi, Sergey I. "Plasmonic nano-guides and circuits." Plasmonics and Metamaterials. Optica Publishing Group, 2008.
[2] Davis, Timothy J., Daniel E. Gómez, and Ann Roberts. "Plasmonic circuits for manipulating optical information." Nanophotonics 6.3 (2017): 543-559.
[3] Koch, Ueli, et al. "A monolithic bipolar CMOS electronic–plasmonic high-speed transmitter." Nature Electronics 3.6 (2020): 338-345.
[4] Tuniz, Alessandro. "Nanoscale nonlinear plasmonics in photonic waveguides and circuits." La Rivista del Nuovo Cimento 44.4 (2021): 193-249.
[5] Cao, Yang, et al. "Add drop multiplexers for terahertz communications using two-wire waveguide-based plasmonic circuits." Nature Communications 13.1 (2022): 4090.
[6] Kirchain, Randolph, and Lionel Kimerling. "A roadmap for nanophotonics." Nature Photonics 1.6 (2007): 303-305.
[7] Abdulnabi, Saif Hasan, and Mohammed Nadhim Abbas. "Design an all-optical combinational logic circuits based on nano-ring insulator-metal-insulator plasmonic waveguides." Photonics. Vol. 6. No. 1. MDPI, 2019.
[8] Fu, Yulan, et al. "All-optical logic gates based on nanoscale plasmonic slot waveguides." Nano letters

12.11 (2012): 5784-5790.

[9Abdulnabi, Saif H., and Mohammed N. Abbas. "All-optical logic gates based on nanoring insulator–metal–insulator plasmonic waveguides at optical communications band." Journal of Nanophotonics 13.1 (2019): 016009-016009.

[10] El Haffar, Rida, et al. "All-optical logic gates using a plasmonic MIM waveguide and elliptical ring resonator." Plasmonics (2022): 1-12.

[11] Rakhshani, Mohammad Reza, Alireza Tavousi, and Mohammad Ali Mansouri-Birjandi. "Design of a plasmonic sensor based on a square array of nanorods and two slot cavities with a high figure of merit for glucose concentration monitoring." Applied optics 57.27 (2018): 7798-7804.

[12] Enoch, Stefan, Romain Quidant, and Gonçal Badenes. "Optical sensing based on plasmon coupling in nanoparticle arrays." Optics express 12.15 (2004): 3422-3427.

[13] Tao, Jin, Qi Jie Wang, and Xu Guang Huang. "All-optical plasmonic switches based on coupled nano-disk cavity structures containing nonlinear material." Plasmonics 6 (2011): 753-759.

[14] Nozhat, N., and N. Granpayeh. "All-optical nonlinear plasmonic ring resonator switches." Journal of Modern Optics 61.20 (2014): 1690-1695.

[15] Min, C., et al. "Beam focusing by metallic nano-slit array containing nonlinear material." Applied Physics B 90 (2008): 97-99.

[16] Dickson, Robert M., and L. Andrew Lyon. "Unidirectional plasmon propagation in metallic nanowires." The Journal of Physical Chemistry B 104.26 (2000): 6095-6098.

[17] Chen, Jianjun, et al. "Plasmonic Y-splitters of high wavelength resolution based on strongly coupled-resonator effects." *Plasmonics* 7 (2012): 441-445.

[18] Lu, Hua, et al. "Multi-channel plasmonic waveguide filters with disk-shaped nanocavities." Optics Communications 284.10-11 (2011): 2613-2616.

[19] Qi, Yunping, et al. "Theoretical study of a multichannel plasmonic waveguide notch filter with double-sided nanodisk and two slot cavities." Results in physics 14 (2019): 102506.

[20] Alam, M. Z., et al. "Compact low loss and broadband hybrid plasmonic directional coupler." Optics Express 21.13 (2013): 16029-16034.

[21] Guo, Yinghui, et al. "Transmission characteristics of the aperture-coupled rectangular resonators based on metal–insulator–metal waveguides." Optics Communications 300 (2013): 277-281.

[22] Azar, Milad Taleb Hesami, et al. "Design of a high-performance metal–insulator–metal plasmonic demultiplexer." Journal of nanophotonics 11.2 (2017): 026002-026002.

[23] Rah, Yoonhyuk, et al. (2019) 'Optical analysis of the refractive index and birefringence of hexagonal boron nitride from the visible to near-infrared', Optics letters, 44.15: 3797-3800.

[24] Johnson, P.B.; Christy, R.W., "Optical constants of the noble metals," Phys. Rev. 1972, 6, 4370–4379.

[25] D. Choi et al., "Plasmonic optical interference," Nano Lett. 14(6), 3374–3381 (2014).

[26] W. Chen, R. L. Nelson, and Q. Zhan, "Geometrical phase and surface plasmon focusing with azimuthal polarization," Opt. Lett. 37(4), 581–583 (2012).

[27] Kumar, Upkar. Plasmon logic gates designed by modal engineering of 2-dimensional crystalline metal cavities. Diss. Université Paul Sabatier-Toulouse III, 2017.

[28] Ma, Song, et al. "Tunable Size Dependence of Quantum Plasmon of Charged Gold Nanoparticles." *Physical Review Letters* 126.17 (2021): 173902.

[29] Unser, Sarah, et al. "Localized surface plasmon resonance biosensing: current challenges and approaches." *Sensors* 15.7 (2015): 15684-15716.

[30] Mustafa, S. M., Karimi, G., Malek Shahi, M. R., & Abdulnabi, S. H. (2023). Nanomaterials in Nanophotonics Structure for Performing All-Optical 2× 1 Multiplexer Based on Elliptical IMI-Plasmonic Waveguides. *Nanomaterials and Nanotechnology*, *2023*(1), 7790674.

[31] Azzazi, Abdulilah, and Mohamed A. Swillam. "Nanoscale highly selective plasmonic quad wavelength demultiplexer based on a metal–insulator–metal." Optics Communications 344 (2015):

106-112.

[32] Pooja Chauhan, Rukhsar Zafar, "Plasmonic De-multiplexer with High Contrast ratio using Metal-Insulator-Metal Waveguide", SKIT Research Journal, 9, 2, 2019.

[33] Khani, Shiva, Ali Farmani, and Ali Mir. "Reconfigurable and scalable 2, 4-and 6-channel plasmonics demultiplexer utilizing symmetrical rectangular resonators containing silver nano-rod defects with FDTD method." Scientific Reports 11.1 (2021): 13628.